PSFC/JA-01-31

An Experimental and Theoretical Study of the "Quasi-Coherent Fluctuations" in a High Density Tokamak Plasma

Mazurenko, A., Porkolab, M., Mossessian, D., Snipes, J.A.
Xu, X.Q.,* Nevins, W.M.*

November 2001

Plasma Science and Fusion Center
Massachusetts Institute of Technology
Cambridge MA 02139 USA

*Lawrence Livermore National Laboratory,
Livermore, CA 94551

This work was supported by the US Department of Energy, MIT Grant No. DE-FC02-99ER54512 and the Lawrence Livermore National Laboratory under Contract No. W-7405-ENG-48.

Submitted for publication in *Physical Review Letters*.

Abstract

The Quasi-Coherent (QC) mode, observed at high densities during enhanced D-alpha (EDA) H-Mode in the Alcator C-Mod tokamak, has been studied with a phase contrast imaging (PCI) diagnostic. The QC mode is believed to be responsible for the reduced particle (and impurity) confinement during H-mode operation, so as to allow quasi-steady state operation of the tokamak**.** It is proposed that the QC mode is a form of resistive ballooning mode known as the resistive X-point mode. The measured dispersion and mode stability are found to be in good agreement with the resistive X-point mode predicted by the BOUT (Boundary Plasma Turbulence) code.

The High-Confinement (H-Mode) regime in magnetically confined high temperature plasmas in toroidal configurations is characterized by a significant increase in the energy confinement time (as compared to L-mode, or low-confinement) due to the formation of a transport barrier at the plasma edge [1]. Depending on operating conditions, different types of H-modes have been observed. The ELM-free (Edge Localized Mode) H-mode is free of any large scale MHD instability at the edge; however high-Z impurity accumulation in the plasma core eventually leads to a radiative collapse [2]. ELMy H-mode plasmas are periodically cleansed from impurities; however during the periodic occurrence of ELMs a large fraction of the stored energy is ejected across the plasma edge, leading to undesirably large divertor heat loads [3].

In the high density, compact, diverted Alcator C-Mod tokamak at MIT, yet another kind of H-mode is observed, the enhanced D_α (EDA) H-mode [2]. The plasma in this regime is characterized by significantly reduced impurity confinement compared to the ELM-free H-mode, with only marginally lower energy confinement. The EDA H-mode is an excellent candidate for long pulse or steady state operation owing to the absence of both excessive central radiation and large ELMs. Importantly, the EDA H-mode is found to be always accompanied by a continuous, high frequency (~100kHz) "quasi-coherent" (QC) fluctuation, localized in the steep density gradient in the edge region (pedestal). The QC mode is believed to be responsible for the moderately low particle (and impurity) confinement in the EDA H-mode.

A very similar mode was found earlier on the neutral beam heated PDX tokamak [4]. That mode and the QC mode found on Alcator C-Mod share many characteristics, such

as narrow frequency spectrum, similar $\delta n/n$ and $\delta B/B$ amplitudes, and localization in the plasma edge region. We note that in the neutral beam heated PDX the fluctuations were always bursty in time, whereas in C-Mod typically the QC mode is continuous (although a bursty mode has been observed in special cases). Due to the absence of detailed measurements of the poloidal wave number of the mode on PDX, and a lack of comparison with appropriate theory, an identification of the mode was not possible. In the Alcator C-Mod tokamak, the QC mode is observed by several diagnostics, including phase contrast imaging, a reflectometer, and scanning Langmuir and magnetic probes [5].

In this paper we present detailed measurements of the QC mode using the phase contrast imaging (PCI) diagnostic and comparisons with theoretical predictions. The PCI measures line integrated density fluctuations along 12 vertical chords (Fig. 1). The chords are spaced 3mm apart, making the PCI sensitive to fluctuations that have a wave-number k_R across the laser beam in the range $1.5\ cm^{-1} < |k_R| < 10\ cm^{-1}$ The typical wave-number of the QC mode is found to be $k_R \sim 3\text{-}6 cm^{-1}$. The PCI lacks vertical localization capabilities, being sensitive to Fourier components of the density fluctuations having $k_Z \approx 0$. However, it was found from reflectometer [6] and scanning probe measurements [7] that the mode is localized in the plasma edge within the steep density gradient ("pedestal") region. The poloidal wave-number of the mode, k_θ, may be related to k_R using the condition that $k_Z \approx 0$, so that $|k_\theta| \approx |k_R| \sin\zeta \sim 3\text{-}5 cm^{-1}$ where ζ is the angle

between the separatrix and the vertical at the locations where the PCI cords cross the plasma edge.

The time evolution of the mode frequency spectrum is shown in Fig. 2. Typically, the QC mode starts at 200-250 kHz following the transition from the "low-confinement" (L-mode) to the EDA H-mode and then sweeps down to a steady state value of 60-120 kHz. The spectrum is quite narrow at all times with $\Delta f/f \sim 0.05\text{-}0.2$ (full width at half maximum). The time scale for this transition is about 50 ms (comparable to the toroidal momentum confinement time). The mode wave-number as well as the major pedestal parameters vary by less than 20% during this frequency sweep. This suggests that the observed frequency change is caused primarily by the Doppler shift together with changes in edge plasma poloidal rotation, while the mode's "intrinsic" frequency stays constant in the plasma frame. Occasionally, the mode frequency fluctuates by as much as 30% in concert with sawtooth oscillations in the electron temperature. These frequency fluctuations may result from either changes in pedestal parameters or changes in the edge plasma rotation brought on by the sawtooth crash.

The dispersion relationship, $\omega(k_R)$, measured by the PCI diagnostic is shown in Fig. 3. The QC mode shows up as the two strong peaks at f=95 kHz and k_R=-4 and +5 cm^{-1} (the horizontal resolution is limited by the number of integration chords to 1.6 cm^{-1}). The mode propagates in the electron diamagnetic drift direction, as was found by correlating signals from two Langmuir probes momentarily inserted (a scanning probe) into the plasma edge [7]. The presence of two peaks in the spectrum may be explained by the fact that as the PCI laser beam crosses the plasma vertically, it detects poloidally propagating

edge fluctuations both at the top (generating the PCI signal at negative k_R) and at the bottom (generating the PCI signal at postive k_R) [8].

The typical QC mode poloidal wavenumber inferred from the PCI diagnostic is $k_\theta \sim 4\ cm^{-1}$, which corresponds to a relatively high poloidal mode number of m~100. Higher harmonics of the mode typically are not detected, suggesting that the fluctuation is sinusoidal. This is in contrast to the Edge Harmonic Oscillations [EHO] observed in the DIII-D tokamak where many harmonics are typically seen [9].

The magnetic component of the QC fluctuation has been measured with a coil in the tip of a scanning probe [10]. This coil was oriented to measure the poloidal component of δB. When positioned within ~2 cm of the separatrix during an EDA H-mode the coil detected the QC mode. The peak measured rms amplitude of the fluctuations is ~1.5 G, or about 0.004% of the total magnetic field. Because of the high wave-number of the QC mode the magnetic perturbations fall off rapidly away from pedestal where the mode is localized.

It has been suggested that the QC mode is a resistive ballooning mode [11]. We believe that the QC mode may be a particular form of resistive ballooning mode known as the resistive X-point mode [12,13]. We investigate this hypothesis through detailed comparison between the experimental results and the recently developed Boundary Plasma Turbulence code (BOUT)[12]. BOUT models radially localized boundary-plasma turbulence in realistic divertor geometry using the Braginskii equations for the

evolution of plasma vorticity, density (n_i), electron and ion temperatures (T_e, T_i) and parallel momentum. Although BOUT contains many sources of free energy which can drive plasma turbulence, it has been found that the dominant instability is the resistive X-point mode (a resistive ballooning mode which is strongly influenced by the magnetic geometry near the X-point). Magnetic curvature is the dominant instability drive for the resistive X-point mode. This mode is electromagnetic at the outboard midplane ($\partial\phi/ds \approx i\omega A_{||}$) and transitions to an electrostatic resistive mode ($A_{||} \approx 0$) near the X-point. This transition is allowed because the line-bending term is overcome by the electron dissipation and inertia (collisional and collisionless skin effects), proportional to $k_\perp^2$, which become large near the X-point where magnetic shear yields large radial wavenumber, k_r while $B_\theta \rightarrow 0$ yields large k_θ [13].

We start our BOUT simulations using an EDA H-mode plasma profile corresponding to the time slice at 976 ms of the C-Mod discharge 1001020014. The magnetic geometry is obtained from the magnetic equilibrium code EFIT [14], which is run on a 129x129 grid and includes the bootstrap current contribution. This is the same C-Mod discharge shown earlier in Figs. 2 and 3. The equilibrium plasma profiles are obtained by using hyperbolic tangent fits to the experimentally determined plasma density n_e and electron temperature T_e. The mid-plane temperature and density on the separatrix are T_e=50 eV, and n_e=1.2x10^{20} m^{-3}, respectively, while at the top of the pedestal, T_e=300 eV and n_e=4x10^{20} m^{-3}. For these parameters ν^* varies from 5 to several hundred for both

electrons and ions in the boundary region (ψ_n > 95%), and the mean free path for electron-ion collisions, is less than the connection length ($q_{95}R_0 \approx 230$ cm) over the entire simulation volume — varying from 230 cm at the boundary between the BOUT simulation volume and the plasma core (~1 cm inside the separatrix at the outboard midplane) to 3.5 cm in the far scrape-off layer (~1 cm outside the separatrix at the outboard midplane). This high collisoniality justifies both the assumption $T_i \approx T_e$ and the Braginskii fluid equations, which are the basis of the BOUT simulation code.

During the first 15 μs of the simulation we observe linear growth of a classic resistive X-point mode [13] (that is, a linear instability localized along the magnetic field by dissipation at the X-points with a radial extent less than the pedestal width) at a frequency f≈400 kHz, with growth rate $\gamma_{lin} \approx 6\times10^5 s^{-1}$ and midplane poloidal wavenumber $k_\theta \approx 5 cm^{-1}$. Over the following 20μs the instability saturates, there is an inverse cascade to longer wavelength, and the radial electric field evolves to a self-consistent, steady-state profile.

We observe a remarkably coherent resistive X-point mode over the final 100 μs of the simulation. This mode has a radial scale length for the scalar and vector potentials which is greater than the width of the pedestal. In this respect, it resembles the surface wave described by Rogers and Drake [15]. In particular, after the inverse cascade the poloidal wavenumber at the outboard midplane is in reasonable agreement with their estimate, $k_\theta \approx (\rho_s^2 R)^{-1/3} \approx 1.45\ cm^{-1}$.

Figure 4 shows the radial profiles from the BOUT simulation of the equilibrium density, the rms density fluctuation, the rms magnetic field fluctuation, and the radial electric field at the outboard midplane. The density fluctuations and the E_r well are localized about the maximum density gradient in the edge pedestal — about 2 mm inside the separatrix in these simulations. The rms density fluctuation at the pedestal midpoint has a relative amplitude of 36% with a full width at half maximum of 5 mm, while the rms fluctuating potential is about 80 V at the same location. The peak amplitude of the fluctuating poloidal magnetic field seen in BOUT is 20 Gauss — 0.05% of the total magnetic field at the outboard midplane. The magnetic perturbation falls off rapidly within the plasma scrape-off layer, reaching a value of ~1 Gauss at a distance of 1 cm from the separatrix. Similar rms values of δB_θ at this location have been observed on magnetic probes [10].

The BOUT simulations also supports our interpretation that the downward sweep in the quasi-coherent mode frequency observed in Fig. 2 results from a change in the edge plasma rotation velocity. In a sequence of BOUT simulations the frequency of the quasi-coherent mode varied from 400 to 40 kHz as the plasma rotation velocity at the boundary between the BOUT simulation volume and the core plasma was varied from –3 km/s to +9km/s (corresponding to radial electric fields from –13 kV/m to +40 kV/m). Such large radial electric fields have been inferred near the C-Mod plasma edge in past

experiments [16]. In Figs. 4 and 5 we show results from a member of this sequence in which the plasma rotation velocity at this boundary is 5.3 km/s (corresponding to a radial electric field of 22 kV/m) because this choice of the core rotation velocity reproduces the observed quasi-coherent mode frequency, f≈100 kHz.

The (radially averaged) dispersion relation of the density fluctuations from the BOUT simulation at the outboard midplane is shown in Fig. 5. A coherent mode is observed with poloidal wavenumber, $k_\theta = -1.3$ cm^{-1} (the negative value indicates a mode propagating in the electron diamagnetic direction, in agreement with the experiment), frequency f=100 kHz and linewidth Δf≈20 kHz (limited by the length of the data). The poloidal wavenumber is in agreement with the published probe data [7,10], while the frequency and linewidth are essentially the same as those seen by the PCI (see Fig. 2). It follows [13] from the conservation of toroidal mode number and the relation $k_\phi = n/R$ that the poloidal wavenumber, k_θ, for ballooning modes (for which $\boldsymbol{k}\cdot\boldsymbol{B}\approx 0$, or $k_\theta B_\theta \approx -k_\phi B_\phi$) varies within a flux surface as $k_\theta(\theta_1)/k_\theta(\theta_2) \approx [B_\theta(\theta_2)R_2^2]/[B_\theta(\theta_1)R_1^2]$. That is, $k_\theta = -2.6$ cm^{-1} at the top PCI scattering location and $k_\theta = -2.8$ cm^{-1} at the bottom PCI scattering location. Recalling that the PCI diagnostic is sensitive to the components of the density fluctuation with $k_Z \approx 0$, so that $|k_R| \approx |k_\theta|/\sin\zeta$, the corresponding values of k_R are –3.2 cm^{-1} and +3.6 cm^{-1} respectively, in reasonable agreement with the PCI measurements. The difference

between the measured and calculated k_θ is mainly due to discreteness of k_θ in the BOUT simulations. It is expected that with a bigger simulation volume the value of k_θ observed in the BOUT simulations would increase by as much as 50%.

In conclusion, we have presented experimental measurements of the dispersion relation of the Quasi-Coherent (QC) mode by a non-intrusive diagnostic. The measured dispersion and stability of the QC mode is in good agreement with the resistive X-point mode predicted by the BOUT (Boundary Plasma Turbulence) code. Future studies will include a comparison of the dependence of the QC mode on plasma shaping and safety factor q [2,5] with BOUT simulations.

The authors would like to acknowledge the efforts of the entire Alcator C-Mod group in carrying out the experiments reported here. In particular, we are thankful to Y. Lin and B. LaBombard for the reflectometer and the scanning probe data, respectively, and to R.H. Cohen, J. Drake, M. Greenwald, B. Rogers, T.D. Rognlien, D.D. Ryutov, and S. Wolfe for valuable discussions. This work was performed under the auspices of the US Department of Energy at MIT under Contract No. DE-FC02-99ER54512, and at the Lawrence Livermore National Laboratory under Contract No. W-7405-ENG-48.

REFERENCES

[1] W. Suttrop, Plasma Phys. Control. Fusion **42**, A1 (2000).

[2] M. Greenwald *et al.,* Phys. Plasmas **6**, 1943 (1999).

[3] H. Zohm, Plasma Phys. Controlled Fusion **38**, 105 (1996).

[4] R.E. Slusher *et al.,* Phys. Rev. Lett. **7**, 667 (1984).

[5] E. Marmar *et al.,* in Plasma Physics and Controlled Nuclear Fusion Research, Proc. 18th Int. Conf. Sorrento, 2000, IAEA-CN-77/EX2/5.

[6] Y. Lin *et al.,* Rev. Sci. Instrum. **70**, 1078 (1999).

[7] A.E. Hubbard *et al.,* Phys. Plasmas **8**, 2033 (2001).

[8] A. Mazurenko, Ph.D. Thesis, MIT Department of Physics, 2001.

[9] K.H. Burrell *et al.*, Phys. Plasmas **8**, 2153 (2001).

[10] J.A. Snipes *et al.,* Plasma Phys. Cont. Fusion **43**, L23 (2001).

[11] B.N. Rogers, J.R. Drake, and A. Zeiler, PRL **81**, 4396 (1998).

[12] X.Q. Xu. *et al.*, Phys. Plasmas **7,** 1951 (2000).

[13] J. Myra *et al.*, Phys. Plasmas **7**, 4622 (2000).

[14] L.L. Lao *et al.*, Nucl. Fusion **25**, 1611 (1985).

[15] B.N. Rogers, J.R. Drake, Phys. Plasmas **6**, 2797 (1999).

[16] I.H. Hutchinson *et al.*, Plasma Phys. and Controlled Fusion **41**, A609 (1999).

Figure Captions

FIGURE 1. Experimental setup and plasma cross section of C-Mod. The laser beam of the PCI diagnostic passes vertically through the plasma to a phase plate and a detector array (not shown). The arrows depict the location and the direction of propagation of the QC mode.

FIGURE 2. Time sequence showing the QC mode starting at about 0.79 sec following an L-H transition. Also shown are traces of central T_e and the D_α emission line intensity.

FIGURE 3. Two-dimensional spectrum of the 12 PCI signals. Positive k_R correspond to fluctuations propagating across the PCI beam in the direction of increase of major radius R, negative k_R - in the direction of decrease of R. Two separate peaks for QC mode appear since the mode is detected twice - once on the top and once at the bottom of the plasma.

FIGURE 4. Radial profiles of background plasma density, (rms) density perturbation, (rms) poloidal magnetic field perturbation, and radial electric field at outboard midplane.

FIGURE 5. The radially averaged dispersion relation from the BOUT simulation for density fluctuations at the outboard midplane showing a coherent mode at $k_\theta \approx -1.3$ cm^{-1} together with a weaker mode at $k_\theta \approx 2.5$ cm^{-1}. These secondary modes were absent in most BOUT simulations from our E_r-scan.

Figure 1

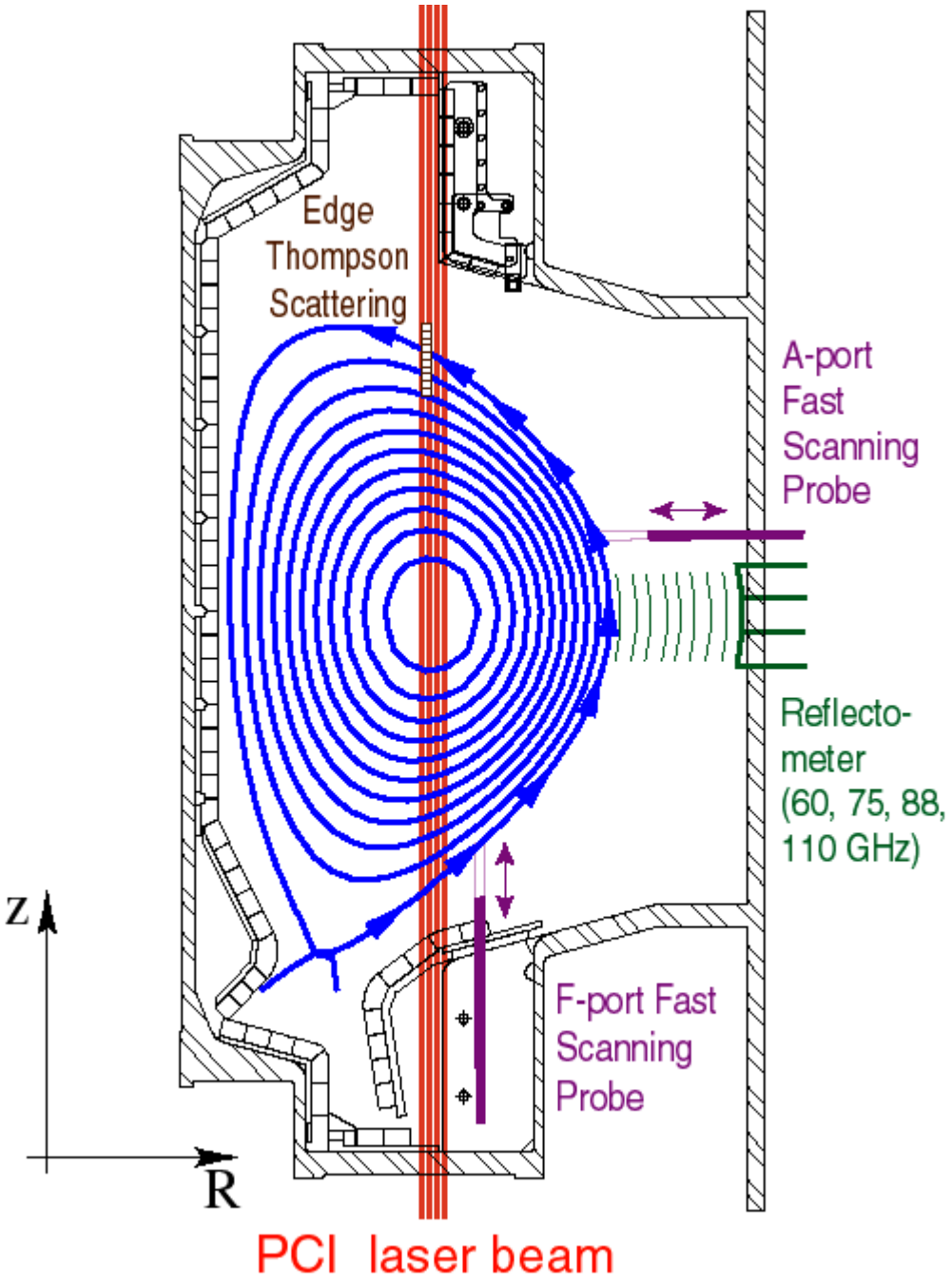
Edge
Thompson
Scattering
A-port
Fast
Scanning
Probe
Reflecto-
meter
(60, 75, 88,
110 GHz)
F-port Fast
Scanning
Probe
Z
R
PCI laser beam

Figure 2

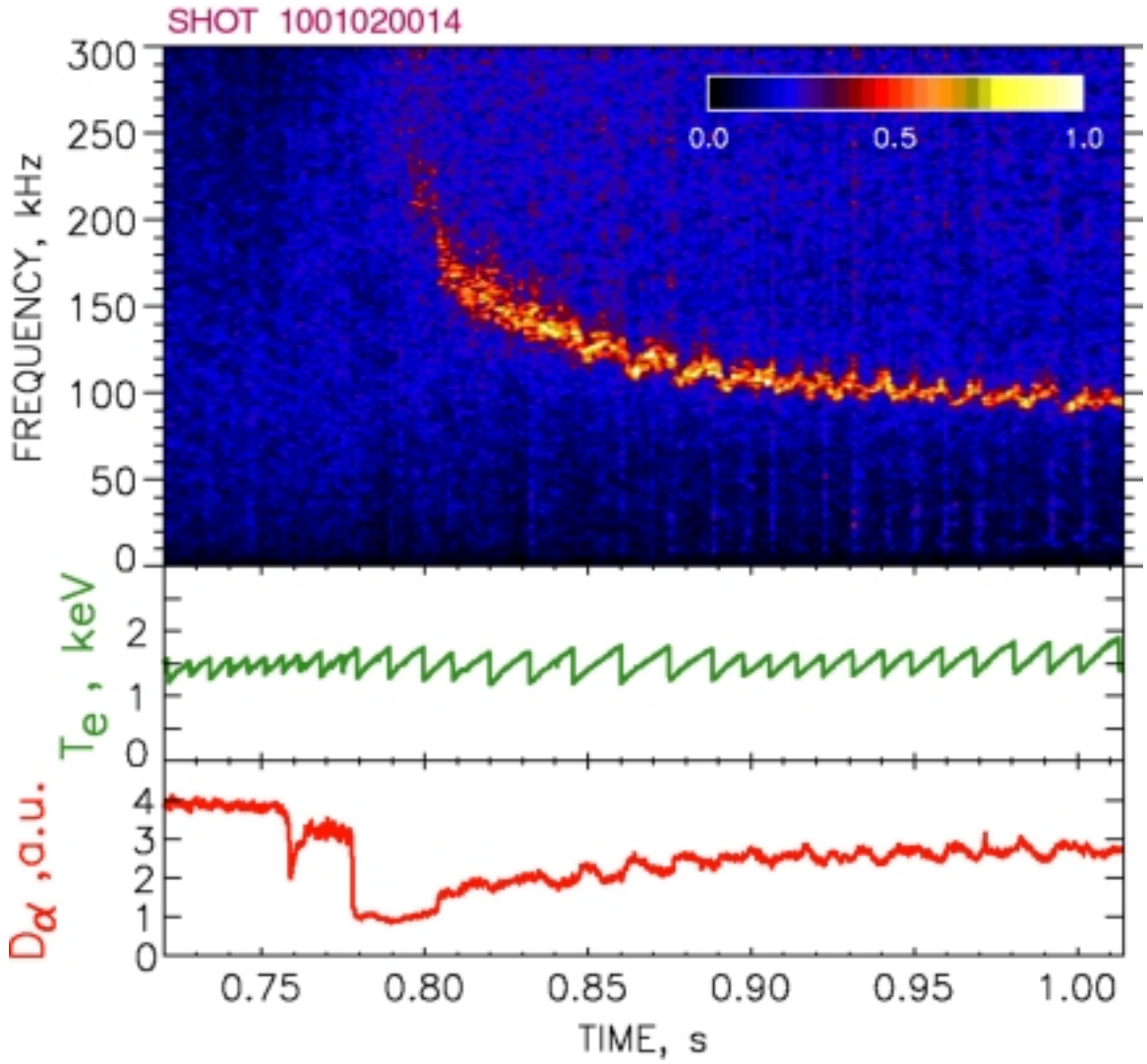
SHOT 1001020014
FREQUENCY, kHz
300
250
200
150
100
50
0
0.0
0.5
1.0
Te , keV
2
1
0
Dα ,a.u.
4
3
2
1
0
0.75
0.80
0.85
0.90
0.95
1.00
TIME, s

Figure 3

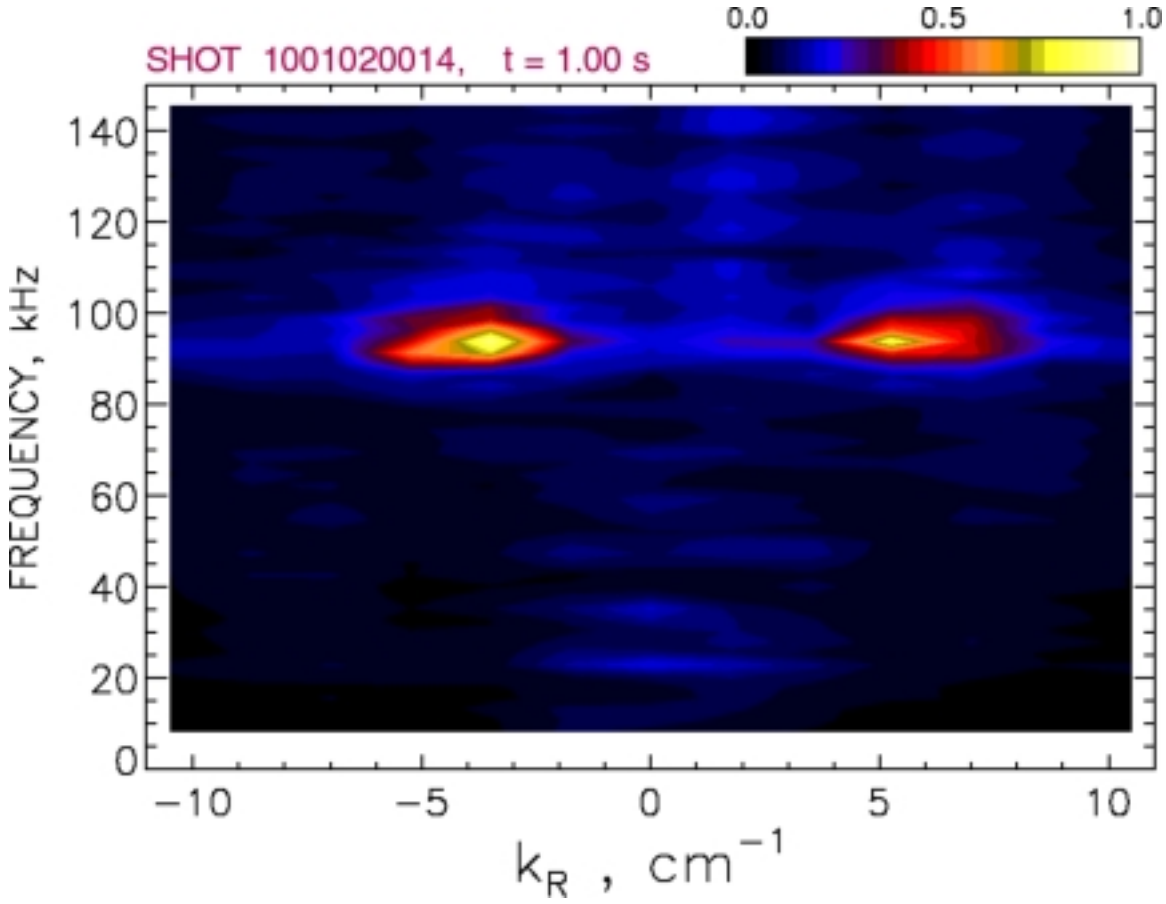
SHOT 1001020014, t = 1.00 s
0.0
0.5
1.0
FREQUENCY, kHz
140
120
100
80
60
40
20
0
−10
−5
0
5
10
k_R , cm^{-1}

Figure 4

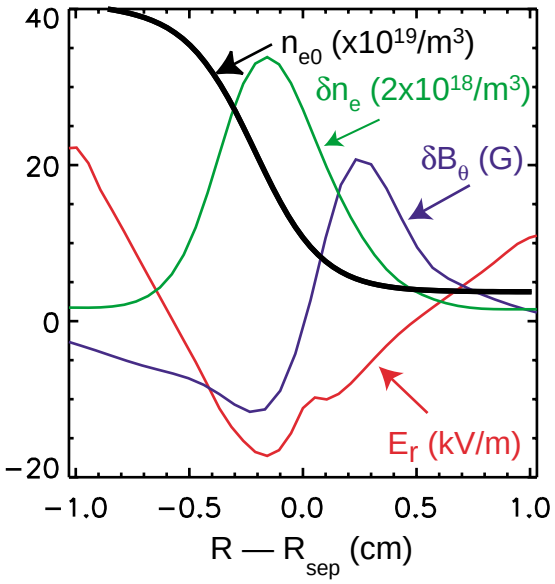
40
20
0
−20
−1.0
−0.5
0.0
0.5
1.0
R — R_sep (cm)
n_e0 (x10^19/m^3)
δn_e (2x10^18/m^3)
δB_θ (G)
E_r (kV/m)

Figure 5

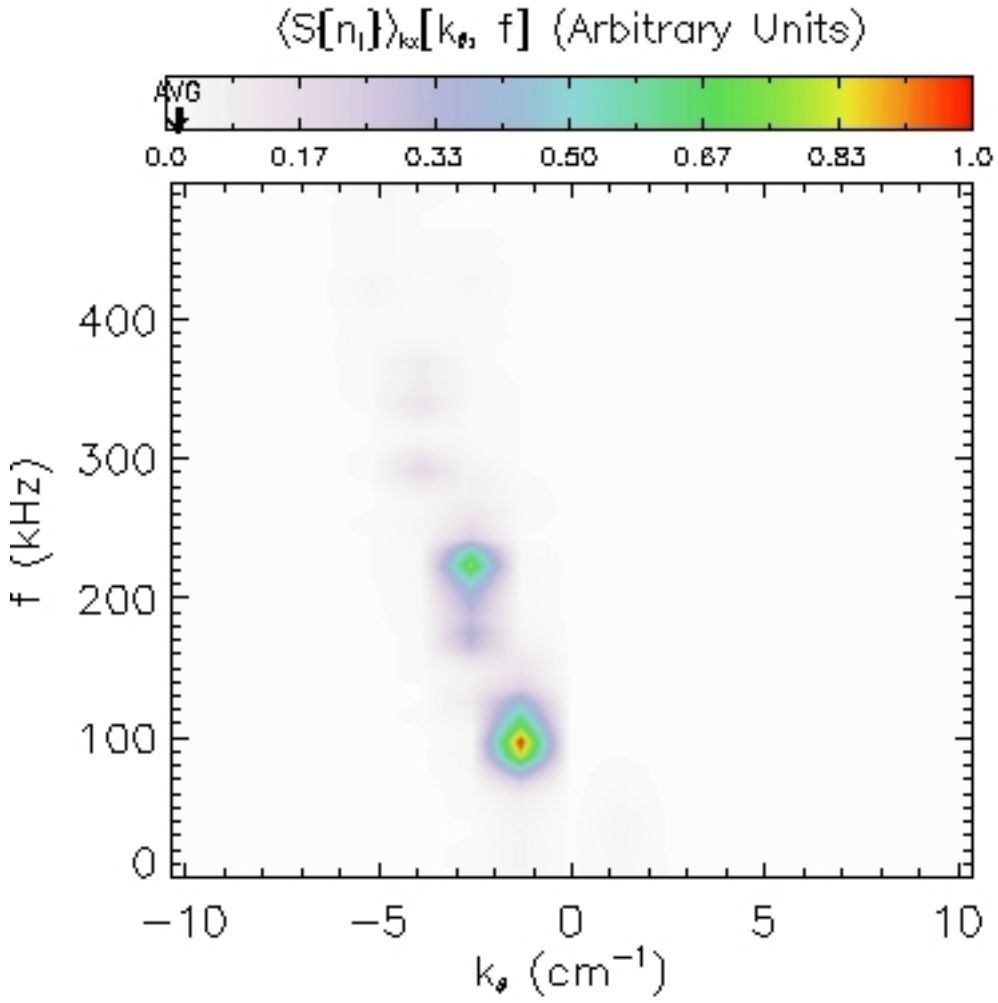
⟨S[n_i]⟩_kx[k_φ, f] (Arbitrary Units)
AVG
0.0
0.17
0.33
0.50
0.67
0.83
1.0
400
300
200
100
0
f (kHz)
−10
−5
0
5
10
k_φ (cm^−1)